Transcriptomics reveal new insights into molecular regulation of nitrogen use efficiency in Solanum melongena

SOCIETY FOR EXPERIMENTAL BIOLOGY

Journal of Experimental Botany
doi:10.1093/jxb/erab121 Advance Access Publication XX XXXX, XXXX

RESEARCH PAPER

Transcriptomics reveal new insights into molecular regulation of nitrogen use efficiency in *Solanum melongena*

Antonio Mauceri[1,†,*], Maria Rosa Abenavoli[1,†], Laura Toppino[2], Sayantan Panda[3], Francesco Mercati[4], Meriem Miyassa Aci[1], Asaph Aharoni[3], Francesco Sunseri[1,*], Giuseppe Leonardo Rotino[2] and Antonio Lupini[1]

[1] Dipartimento Agraria, Università degli Studi Mediterranea di Reggio Calabria, Loc. Feo di Vito snc, Reggio Calabria, Italy
[2] CREA – Research Centre for Genomics and Bioinformatics, Via Paullese 28, Montanaso Lombardo (LO), Italy
[3] Department of Plant and Environmental Sciences, Weizmann Institute of Science, Rehovot, Israel
[4] Istituto di Bioscienze e Biorisorse CNR, Corso Calatafimi 414, Palermo, Italy

[†] These authors contributed equally to this work.
* Correspondence: antonio.mauceri87@unirc.it or francesco.sunseri@unirc.it

Received 22 December 2020; Editorial decision 4 March 2021; Accepted 11 March 2021

Editor: Björn Usadel, Forschungszentrum Jülich, Germany

Abstract

Nitrogen-use efficiency (NUE) is a complex trait of great interest in breeding programs because its improvement is an approach by which high crop yields can be maintained whilst N supply is reduced. In this study, we report a transcriptomic analysis of four NUE-contrasting eggplant (*Solanum melongena*) genotypes following short- and long-term exposure to low N, to identify key genes related to NUE in the roots and shoots. The differentially expressed genes in the high-NUE genotypes are involved in the light-harvesting complex and receptor, a ferredoxin–NADP reductase, a catalase and *WRKY33*. These genes were then used as bait for a co-expression gene network analysis in order to identify genes with the same trends in expression. This showed that up-regulation of *WRKY33* triggered higher expression of a cluster of 21 genes and also of other genes, many of which were related to N-metabolism, that were able to improve both nitrogen uptake efficiency and nitrogen utilization efficiency, the two components of NUE. We also conducted an independent *de novo* experiment to validate the significantly higher expression of *WRKY33* and its gene cluster in the high-NUE genotypes. Finally, examination of an Arabidopsis transgenic *35S::AtWRKY33* overexpression line showed that it had a bigger root system and was more efficient at taking up N from the soil, confirming the pivotal role of *WRKY33* for NUE improvement.

Keywords: Aubergine, coordinated gene network (CGN), eggplant, ferredoxin–NADP reductase (FNR), light reaction complex genes (LHCs), nitrogen use efficiency (NUE), RNAseq, *Solanum melongena*, transcriptomic, *WRKY33*.

Introduction

Eggplant (aubergine, *Solanum melongena*) is the third most economically important solanaceous vegetable crop, after potato and tomato. It is cultivated worldwide, mainly in China and India, with 54.1 million tons of agricultural production in 2018 (http://faostat.fao.org).

Eggplant breeding has been focused on the improvement of agronomic traits such as yield potential, biotic stress tolerance, and traits related to post-harvest processing (Prohens *et al.*, 2013; Portis *et al.*, 2014; Rotino *et al.*, 2014; Lo Scalzo *et al.*, 2016; Toppino *et al.*, 2016). By contrast, few efforts have been made in breeding programs towards improving nitrogen use efficiency (NUE), despite the fact that eggplant cultivation requires a large amount of nitrogen fertilizer (Pal *et al.*, 2002).

Application of nitrogen (N) fertilization has long been an essential tool to maximize crop yields and quality, particularly for vegetables (Greenwood *et al.*, 1990). However, excess use of N has an economic cost and has caused environmental problems, such as fresh water and air pollution, and damage to human health (Nosengo, 2003; West *et al.*, 2014). One means to overcome this is the selection of crop genotypes with improved NUE. A key first approach for breeding high-NUE crops is the exploitation of genetic variation for this trait in germplasm collections, including older varieties and landraces (Chardon *et al.*, 2010; Hawkesford, 2012; Abenavoli *et al.*, 2016).

NUE is a complex trait defined as the total biomass (or yield) per unit N supplied (Moll *et al.*, 1982), and it is controlled by intricate gene networks involved in N uptake, assimilation, and remobilization, which are in turn influenced by interacting environmental factors. NUE is usually divided in two main components: nitrogen uptake efficiency (NUpE), defined as the ability of the plant to take up N from the soil, and nitrogen utilization efficiency (NUtE), which encompasses the ability of the plant to assimilate, transfer, and utilize N to the harvestable part of the crop (Good *et al.* 2004; Xu *et al.* 2012).

NUpE can be improved by a more efficient root system, and this includes traits such as deeper roots, greater proliferation, and increased lateral root length that enable the plant to increase exploration of soil and to respond to local and systemic N signals, especially under low N supply (Garnett *et al.*, 2009; Lynch, 2013; Qin *et al.*, 2019). An efficient root architecture, associated with efficient nitrate and ammonium transporters (NRTs and AMTs, respectively), will confer higher NUpE to the plant (Xu *et al.*, 2012; Ferrante *et al.*, 2017). Enhancing NUtE is a much more complex task, and it encompasses complex signaling and regulatory mechanisms of N metabolism, translocation, remobilization, C/N balance, and organ senescence (Good *et al.*, 2004; Chardon *et al.*, 2012; McAllister *et al.*, 2012; Xu *et al.*, 2012; Tegeder *et al.*, 2018). Hence, a better understanding of the biochemical, physiological, and molecular mechanisms that regulate NUE and its components will be useful for breeding (Good *et al.*, 2004; Xu *et al.*, 2012; He *et al.*, 2015; Ferrante, *et al.*, 2017).

Many transcription factors (TFs) and protein kinases (PK) have recently been identified in crop plants as key genes that can influence nitrogen uptake, assimilation, translocation, and remobilization (Masclaux-Daubresse *et al.*, 2010; Kant *et al.*, 2011; Xu *et al.*, 2012; Simons *et al.*, 2014). Among the TF families, *WRKY* is one of the largest, and its members harbor a highly conserved domain of 60 amino acid residues (Eulgem *et al.*, 2000). *WRKY*s are involved in many physiological and developmental processes, as well as in plant responses to both biotic (Eulgem *et al.*, 2000; Rushton *et al.*, 2010) and abiotic stress (Li *et al.*, 2011; Shen *et al.*, 2012; Viana *et al.*, 2018). They are also known to play a mediator role in combined abiotic stress and in cross-talk between biotic and abiotic stress (Banerjee and Roychoudhury, 2015). Overexpression of *WRKY1* and *WRKY33* is reported to increase germination rate and promote root growth in Arabidopsis under different stresses (He *et al.*, 2016).

The development of next-generation sequencing (NGS) has opened up intriguing possibilities by improving the efficiency and speed of gene discovery (Ansorge, 2009). Many studies on crop plants grown under different N conditions have been carried out to identify the expression patterns of N-reactive and NUE-related genes through transcriptomics (Hao *et al.*, 2011; Amiour *et al.*, 2012; Gelli *et al.*, 2014; Simons *et al.*, 2014); however, few studies on differential transcriptomic profiling in eggplant have been reported (Li *et al.*, 2018, 2019; Zhang *et al.*, 2019), and none of them have examined N metabolism and NUE. The availability of three genome drafts for eggplant (Hirakawa *et al.*, 2014; Barchi *et al.*, 2019; Wei *et al.*, 2020) will help with the implementation of genomics and bioinformatics tools to identify differentially expressed genes involved in traits of interest.

We recently investigated several eggplant accessions of different origins grown in both hydroponic and potted soil systems under low and high N supply, and identified four genotypes with contrasting NUE (Mauceri *et al.*, 2020). The aim of the current study was to use these genotypes to identify key genes involved in the ability to cope with N stress under limited supply in both the short and long term. Using an RNA-seq approach, the transcriptomic profiles are compared to determine the key molecular players involved in the plant responses to low nitrate with the aim to identify novel NUE-related target genes. Our results indicated that the transcription factor WRKY33 together with genes related to the light-harvesting complex and to the ferredoxin–NADP reductase appear to be the main factors that trigger networks of genes associated with the low-N response in eggplant.

Materials and methods

Plant materials and experimental design

Four genotypes of eggplant (*Solanum melongena* L.) were used, namely AM22, AM222, 67-3, and 305E40, which possess several contrasting morphological traits (Cericola *et al.*, 2013) and have contrasting NUE (Mauceri *et al.*, 2020). In both hydroponic and glasshouse experiments, AM222 has been shown to be N-use efficient whilst AM22 is inefficient, and 305E40 and 67-3 show an intermediate response to low-N, with 67-3 being more efficient then 305E40 (Mauceri *et al.*, 2020).

Seeds of each accession were germinated in Petri dishes and after 10 d the seedlings were transferred to hydroponic tanks (4 l, 10 seedlings per tank) containing a nutrient solution consisting of 2.5 mM K_2SO_4, 2 mM $MgSO_4$, 1 mM KH_2PO_4, 46 μM H_3BO_3, 9 μM $MnCl_2$, 0.76 μM

$ZnSO_4$, 0.32 μM $CuSO_4$, 0.11 μM Na_2MoO_4, and 20 μM Fe-EDTA (Mauceri *et al.*, 2020). The tanks were placed in a growth chamber at 24 °C, 65% relative humidity, and a 14-h photoperiod with a light intensity of 350 μmol m^{-2} s^{-1}. After 2 d of N deprivation (i.e. seedlings 12 d old), 0.5 mM $Ca(NO_3)_2$ was added to the solution and the seedlings were grown for a further 16 d. The nutrient solution was renewed every 3 d and the pH was adjusted to 5.8 using 1 N KOH every day. Seedlings were harvested midway through the light period before N supply at 12 d old (T0), after 24 h of N supply (T1), and after 16 d of N supply (T2) for RNA-seq of the shoots (i.e. leaves and stems) and the roots. Three biological replicates were used, each of which consisted of the tissues of eight plants bulked together.

Plant nitrogen content and nitrogen use efficiency

Total nitrogen content (N_c, mg) was determined by a combustion method using a CNS-1000 analyser (LECO Instruments Ltd, Mississauga, ON, Canada) as described by Lupini *et al.* (2017). Nitrogen use efficiency (NUE) was calculated as SDW/N%, where SDW is shoot dry weight (g) and N% is the percentage N content of the shoot (Chardon *et al.*, 2010), and nitrogen utilization efficiency (NUtE) was calculated as SDW×SDW/N_c (Siddiqi and Glass, 1981). Nitrogen uptake efficiency (NUpE) was also calculated as the total dry weight (TDW) of the plant (shoot+root) × the N concentration (g N per g TDW) (Chardon *et al.*, 2010).

RNA-sequencing and data analysis

Total RNA was isolated and purified using a Mini RNeasy Plant kit (Qiagen) and Precision DNase (Primer Design). RNA degradation and contamination were monitored on 1% agarose gels and samples were quantified using a NanoDrop 2000 (Thermo Scientific). cDNA libraries were constructed using 500 ng of total RNA per sample, following the TranSeq approach with single-end 60-bp reads as described by Tzfadia *et al.* (2018). Libraries were then sequenced on six lanes of a HiSeq 2500 System (Illumina), using the SR60 protocol. The output was ~3 million reads per sample, meeting the recommendation of Tzfadia *et al.* (2018).

Bioinformatics data analysis

The bioinformatics service for all the downstream analysis was provided by the Mantoux Bioinformatics Institute of Nancy and the Stephen Grand Israel National Center for Personalized Medicine, Weizmann Institute of Science. The sequencing data were subjected to quality control (QC) with FastQC, a tool for high-throughput sequence data (www.bioinformatics.babraham.ac.uk/projects/fastqc).

Poly A/T tails, Illumina sequencing adapters, and GGG bases at the start of read (TranSeq protocol) were trimmed from the sequenced reads using Cutadapt (Martin, 2011). Reads shorter than 30 bp were discarded, and the remainder were mapped to the eggplant reference genome SMEL_V3.2016_11_01 from the Italian Consortium (Barchi *et al.*, 2019) using STAR v. 2.4.2a (with EndToEnd option and outFilterMismatchNoverLmax set to 0.04) (Dobin *et al.*, 2013). Counting proceeded over the transcript end site (TES) region of each gene (where the TES region is defined as 200 bp downstream from the end of each gene, and at least 500 bases upstream to the end of gene), and was annotated in SMEL_V3.2016_11_01 using HTSeq-count (intersection-strict mode) (Anders *et al.*, 2015).

Differential expression analysis was performed using the R package DESeq2 (1.10.1) (Love *et al.*, 2014; Robinson and Oshlack, 2010) with the betaPrior, cooksCutoff, and independentFiltering parameters set to False. Raw *P*-values were adjusted for multiple testing using the procedure described by Benjamini and Hochberg (1995). Pipeline was constructed using Snakemake. The threshold levels for detection of differentially expressed genes (DEGs) were set at a FDR-corrected *P*-value <0.05 and $\log_2$FC >|1| using the method described by Benjamini and Hochberg (1995).

Principal component analysis (PCA) was carried out using PCAGO, an interactive web service that is useful for analysing RNA-seq data to obtain initial characterization of the clustering of biological samples and insights into the biological background of experiments (Gerst and Hölzer, 2019, Preprint).

Overview of the metabolism pathway

Pathway analysis was based on the MapMan ontology (Thimm *et al.*, 2004) and figures were created using the mercator tool (http://mapman.gabipd.org/web/guest/mercator), using the default parameters assigned by the MapMan bin to the eggplant transcripts. $\log_2$-fold changes obtained from the DESeq2 output were used as software inputs to depict expression changes among the different genotypes.

Gene ontology and enrichment analysis

Gene ontology (GO) classifies genes and their products according to the corresponding biological processes (BP), cellular components (CC), and molecular functions (MF). The GO enrichment analysis was performed using the topGO bioconductor package release (v.3.8; http://dx.doi.org/10.18129/B9.bioc.topGO).

Construction and visualization of comparative co-expression networks

The CoExpNetViz tool (http://bioinformatics.psb.ugent.be/webtools/coexpr/) was adopted in order to construct gene co-expression networks able to identify correlations among genes that were simultaneously either up- or down-regulated within the same biological process in one or more genotypes. The analysis was performed using a set of queries or 'bait' genes as input (chosen by the user) and a minimum set of gene expression data (Tzfadia *et al.*, 2016). Based on the Pearson's correlation coefficients (PCCs), the relationships among genes were calculated and co-expressed genes were identified. Genes were considered as being co-expressed when the correlation fell below the 1st or above the 99th percentile of the expression distribution based on the similarity of expression profiles of 4000 random genes and on correlation thresholds lower than the 5th percentile and higher than the 95th percentile. After calculation of the correlation matrices, positive and negative cut-off values (Vandepoele *et al.*, 2009) were used to translate the *r*-values into a graphical form in which nodes and edges represent genes and co-expression relationships, respectively.

Pearson's correlation coefficients between gene networks and phenotypic data

Pearson correlation coefficients between the physiological traits (NUE and its components), morphological traits, and root traits taken from Mauceri *et al.* (2020), and the baits and their related genes were performed using the R package Hmisc (https://cran.r-project.org/web/packages/Hmisc/). Correlation coefficients lower than 0.6 and with a *P*-value equal to or higher than 0.05 were discarded.

RNA-seq data validation by RT-qPCR

To validate the results, the same RNA samples that had previously been utilized for the sequencing experiment were used for gene expression analysis of the most important DEGs by quantitative real-time PCR (qRT-PCR). In addition, an independent hydroponic experiment was

performed using the four genotypes. The same DEGs were examined after a long exposure (T2) to low N (0.5 mM) using two technical and two biological replicates. For this, total RNA was extracted from 100 mg of root and shoot samples using an RNeasy Plant Mini Kit (Qiagen) according to the manufacturer's instructions. The RNA was checked for quantity and quality using a NanoDrop 2000 (Thermo Scientific) and 15 (w/v) agarose gel electrophoresis, and then 500 ng of total RNA was reverse-transcribed using a QuantiTect Reverse Transcription Kit (Qiagen) in a final volume of 20 µl according to the manufacturer's instructions.

Gene expression was analysed using qRT-PCR performed on a StepOnePlus Real-Time PCR System (Applied Biosystems). Each reaction contained 1 µl diluted cDNA (1:10), 0.1 µM each of the forward and reverse gene-specific primers (Supplementary Table S1), and 5 µl SYBR Green qPCR Master Mix (Applied Biosystems) in a final volume of 10 µl. qRT-PCR reactions were performed with three technical and three biological replicates. The thermal cycling program used was as follows: 4 min at 94 °C, 40× cycling for 30 s at 94 °C, 60 s at 59 °C annealing temperature, and 72 °C for 30 s. The specificity of reactions was evaluated by melt-curve analysis and a relative standard curve for each gene was generated using a 3-fold serial dilution of pooled cDNA (obtained by mixing equal proportions of all cDNA samples) using the StepOnePlus Software v.2.3 (Applied Biosystems). PCR efficiency of 10 primer pairs was optimized to be in the range 80–120%.

Primer sequences and PCR efficiency values of all the genes are shown in Supplementary Table S1. Adenine phosphoribosyl transferase (*SmAPRT*) and glyceraldehyde 3-phosphate dehydrogenase (*SmGAPDH*) were used as internal references (Gantasala *et al.*, 2013; Barbierato *et al.*, 2017). The relative expression of each gene was calculated using $2^{-\Delta\Delta CT}$ method as described by Livak and Schmittgen (2001). Scatter plots of Pearson's correlation coefficients between the RNA-seq and qRT-PCR data and for the independent hydroponic experiment were obtained using the R package ggplot2 v.3.5.0. (Wickham, 2010).

Root morphological analysis and NUE assessment for AtWRKY33 transgenic lines

We analysed the *SmWRKY33* sequence in order to find the best orthologue in the Arabidopsis genome (www.arabidopsis.org). A dendrogram was obtained using the multiple-sequence alignments of *WRKY* from Arabidopsis, eggplant *SmWRKY33* from both the Eggplant Genome DataBase (http:///eggplant.kazusa.or.jp) and the Italian Consortium 'The Eggplant Genome Project' (http://ddlab.dbt.univr.it/eggplant/), and tomato *SlWRKY33* (www.solgenomics.net). To determine the conserved motifs among *SmWRKY33* and the orthologous *AtWRKY33* we used the MEME online tool v.5.0.5 (Bailey *et al.*, 2009).

We used the Arabidopsis Col-0 wild-type together with the knockdown (KO) mutant *wrky33-2*, and a *35S::AtWRKY33* overexpression (OE) transgenic line in the Col-0 background, both kindly provided by Prof. S. AbuQamar, Department of Biology, United Arab Emirates University (Sham *et al.*, 2017). The *AtWRKY33*-KO mutant and OE line were first validated for transcript abundance using qRT-PCR, with actin (*AtActin11*) and clathrin (*AtCLT*) as housekeeping genes as described by Sun *et al.* (2010) and Léran *et al.* (2015).

Seeds were surface-sterilized and placed in square Petri dishes (100×150 cm) containing agarised (0.8% w/v) Murashige–Skoog basal medium (Sigma-Aldrich), supplemented with 1% sucrose (pH 6.0). The Petri dishes were then placed vertically in a growth chamber as described by Lupini *et al.* (2013, 2014). After 5 d, the seedlings were exposed to either low nitrate (0.5 mM) or high nitrate (10 mM) nitrate for a further 7 d. Images of the seedlings at 12 d old were acquired by scanning (STD4800, Régent Instruments Canada Inc.). Total root length, primary root length, and lateral root length were measured using the WinRhizo Pro Software v. 2016a, 32-bit version (Régent Instruments). Lateral root number (LRN) was counted manually from the images (Abenavoli *et al.*, 2008; Lupini *et al.*, 2014).

Seeds of the Arabidopsis wild-type, KO mutant, and OE line were also germinated in pots (diameter 7 cm, 110 cm^3 volume; three seeds per pot) filled with a perlite:peat (1:1) substrate, and irrigated every 3 d using the same low- and high-N nutrient solutions. The plants were harvested after 45 d, and N_c and NUE were determined as described above, using three replicates.

Results

In this study we analysed the transcriptomic profiles of four genotypes of eggplant with differing NUEs, namely AM222 and 67-3, which have high values, and 305E40 and AM22, which have low values (Supplementary Fig. S1; Mauceri *et al.*, 2020). The experimental design incorporated sampling at three time points (T0 before N supply; T1 after 24 h of low N supply; and T2 after 16 d of low N supply) of both shoot and root samples collected from plants grown in a hydroponic system.

PCA analysis and identification of differentially expressed genes

Principal component analysis for differential gene expression was conducted and clearly indicated that the main source of variation was associated with genotype at T2 (Fig. 1). The data from younger plants (T0 and T1) clustered together compared to the older ones (T2). In order to detect differentially expressed genes (DEGs), we performed 44 pairwise comparisons (36 between genotypes at the same time-point and eight between each genotype at T1 versus T0), avoiding comparisons of gene expression influenced by the growth stage (T2 versus T1, and T2 versus T0; Supplementary Table S2).

In the roots, the highest number of DEGs was found in the comparison between AM222 and 305E40 at T0 and T2, while at T1 the highest number was detected in the comparison between 67-3 and AM22 (Supplementary Table S2). In the shoots, the highest number of DEGs was found in the comparison between AM222 and 67-3 at T2. A comparison of T1 versus T0 showed that AM22 had the highest number of DEGs in both the roots and shoots. The DEGs were then subject to pathway analysis to give an overview of metabolism and to Gene Ontology classification to identify the up- and down-regulated genes shared by the genotypes.

Metabolic pathways analysis using MapMan

The metabolic pathways induced by N treatment in the roots and shoots were visualized using MapMan analysis by comparing AM22 (the most N-use inefficient genotype in all the experiments; see Mauceri *et al.*, 2020) to each of the other genotypes at each of the three time-points (Supplementary Fig. S2).

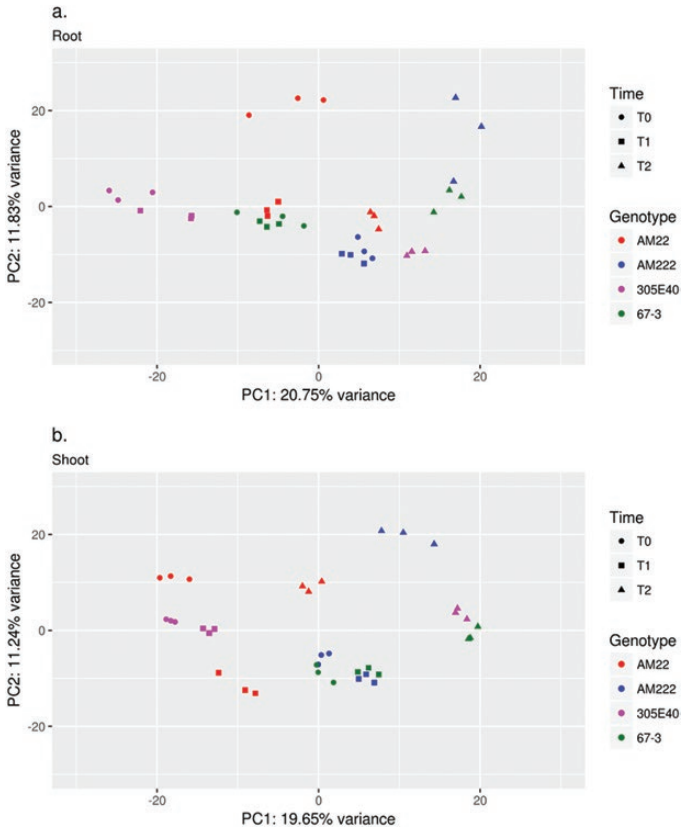

Fig. 1. Principal component (PC) analysis of gene expression in roots (A) and shoots (B) of four eggplant genotypes with differing nitrogen-use efficiency (NUE) subject to low N supply. Following N deprivation for 2 d, seedlings at 12 d old were supplied with 0.5 mM $Ca(NO_3)_2$. Samples were taken immediately prior to the N treatment (T0), after 24 h of treatment (T1), and after 16 d treatment (T2). Details of the comparisons are given in Supplementary Table S2. Comparisons between T1 versus T2 were not made in order to avoid confounding influences of the different growth stages. Under low-N conditions, AM222 has the greatest NUE, followed by 67-3 and 305E40, with AM22 having the lowest NUE (Supplementary Fig. S1).

At T0, the main changes in the roots were observed in transcripts related to cell wall and secondary metabolism in all the paired genotype comparisons, and a prevalent up-regulation of genes was observed in both AM222 and 67-3 compared to AM22 (Supplementary Fig. S2A). At T1, comparable changes were detected although with a decrease in the number of DEGs, and a down-regulation of lipid metabolism genes was observed in both AM222 and 67-3 compared with AM22 (Supplementary Fig. S2B). At T2, significant differences were observed in all the three comparisons for gene expression in phenol and flavonoid pathways (both up- and down-regulation) as well as for genes related to lipid pathways (Supplementary Fig. S2C).

In shoots at T0 there was a down-regulation of genes involved in secondary metabolism (mainly flavonoid and phenols) in the comparisons between AM22 and the three other genotypes (Supplementary Fig. S2D). In addition, a significant up-regulation of genes involved in light reactions, tetra-pyrrole, and N metabolism was apparent in the N-use efficient genotypes AM222 and 67-3 compared to AM22 (Supplementary Fig. S2D). By contrast, only up-regulation of genes involved in the tetra-pyrrole pathway was observed in the comparison between 305E40 and AM22 (Supplementary Fig. S2D). At T1, significant up-regulation of genes related to the light-reaction complex and tetra-pyrrole was observed in all three genotypes compared to AM22 (Supplementary Fig. S2E). At T2, there were noticeable reductions in the numbers of DEGs, but AM222 continued to show significant differences in phenol metabolism compared to AM22 (Supplementary Fig. S2f).

In summary, the RNA-seq data showed that in both the roots and shoots there were considerable differences between the genotypes in cell wall, lipid, and secondary metabolism. Interestingly, in the shoots a considerable number of DEGs were involved in the light-reaction pathway. We therefore examined the most significant DEGs from data intersection in the more N-use efficient genotypes AM222 and 67-3 compared to AM22 and filtered the results according to functional annotation. Five genes showed the highest log_2-fold changes (log_2FC) in value at T0, four at the short-term time-point T1, and one at the long-term time-point T2 (Supplementary Fig. S2). At T1 these genes were related to the light-harvesting complex (LHC) and light receptors, while at T2 an isoform of the ferredoxin–NADP reductase (FNR) was strongly expressed mainly in AM222, the most N-use efficient genotype. By contrast, no significant DEGs were shared in the roots (data not shown).

GO classification of responses to low N supply within genotypes

TopGO enrichment analysis for all the comparisons between the genotypes is shown in Supplementary Table S3. In the roots, differences in GO biological processes were observed in AM222 when comparing T1 to T0, i.e. the short-term response. In particular, transcript enrichment was observed related to the 'response to nitrate' (GO: 0010167), which underlined a significant up-regulation of the genes encoding NRT1/PTR FAMILY 6.3-like, BTB/POZ and TAZ domain-containing protein 1-like (BTB1), the chloride channel protein CLC-b-like (CLC-B), and ferredoxin–nitrite reductase, chloroplastic (NIR1). In addition, genes encoding proteins belonging to 'inorganic anion transport' (GO:0015698) were up-regulated in the N-use efficient genotypes, such as 1-like molybdate transporter (MOT1), transporter-like sulfate, and phosphate transporter, and similarly two isoforms of ferredoxin-chloroplastic-like involved in plant responses to N-stress in 'ferredoxin metabolic process' (GO:0006124) were also up-regulated (Table 1A). In the shoots, AM222 showed significant up-regulation of the chloride channel protein CLC-b-like, the NRT1/PTR FAMILY 6.3-like, and the ferredoxin–nitrite

Table 1. Differentially expressed genes classified within 'biological process' by TopGO enrichment analysis in roots (A) and shoots (B) of the eggplant genotype AM222 in response to low nitrogen supply

Gene	ID	Log_2 fold-change	*P*-value	*P*-adj	GO subcategory
(A) Roots					
NRT1/ PTR FAMILY 6.3-like	SMEL_008g297920.1	4.293	3.88×10^{-23}	1.59E-19	Response to nitrate, inorganic anion transport
BTB/POZ and TAZ domain-containing protein 1-like	SMEL_003g189050.1	3.574	6.56×10^{-9}	1.41E-06	Response to nitrate
Chloride channel protein CLC-B-like	SMEL_002g162840.1	1.727	2.59×10^{-7}	3.42E-05	Response to nitrate, inorganic anion transport
Ferredoxin–nitrite reductase, chloroplastic (NIR1)	SMEL_012g384590.1	1.542	1.09×10^{-6}	0.00012	Response to nitrate
NRT1/ PTR FAMILY 6.3-like	SMEL_008g317030.1	1.322	1.01×10^{-8}	2.06E-06	Response to nitrate, inorganic anion transport
Molybdate transporter 1-like	SMEL_010g356400.1	2.248	1.96×10^{-6}	0.000201	Inorganic anion transport
Sulfate transporter -like	SMEL_006g270520.1	2.034	3.78×10^{-14}	2.58E-11	Inorganic anion transport
Phosphate transporter	SMEL_003g169230.1	1.074	1.59×10^{-3}	0.039113	Inorganic anion transport
Probable ubiquitin-conjugating enzyme e2 24-like	SMEL_000g064800.1	-1.098	1.12×10^{-6}	0.00012	Inorganic anion transport
S-type anion channel SLAH3-like	SMEL_003g183450.1	-1.152	2.24×10^{-3}	0.049937	Inorganic anion transport
Ferredoxin- chloroplastic-like isoform 1	SMEL_000g010460.1	2.352	1.22×10^{-21}	2.49E-18	Ferredoxin metabolic process
Ferredoxin- chloroplastic-like isoform 2	SMEL_004g207860.1	-1.181	1.50×10^{-3}	0.038181	Ferredoxin metabolic process
(B) Shoots					
Chloride channel protein CLC-B-like	SMEL_002g162840.1	1.568	1.43×10^{-7}	3.74E-05	Response to nitrate
Nitrate transporter-like	SMEL_006g256580.1	1.552	1.92×10^{-3}	0.037590	Response to nitrate
Ferredoxin–nitrite reductase, chloroplastic (NIR1)	SMEL_012g384590.1	1.384	1.19×10^{-4}	0.005865	Response to nitrate

Differential expression analysis was performed using the DESeq2 R package (v.1.10.1). The threshold levels for DEG detection were set as a FDR-corrected *P*-value <0.05 and log_2FC >|1|

reductase, chloroplastic (NIR1) genes (GO:0010167) in the short-term response to nitrate (T1 versus T0) (Table 1B). In addition, 'cellular response to toxic substance' (GO:0097237), 'cellular detoxification' (GO:1990748), and 'cellular oxidant detoxification' (GO:0098869) all showed enrichment in the comparison between T1 and T0 comparison in both the 67-3 and 305E40 genotypes, while AM22 showed enrichment in 'response to abiotic stimulus' (GO:0009628) and 'response to inorganic substance' (GO:0010035; Supplementary Table S3). Interestingly, AM222 appeared to be the most reactive to nitrate supply.

GO classification of plant responses to low N supply among genotypes

We then analysed the enrichment of DEGs in both the roots and shoots, adopting the same comparisons employed in the MapMan analysis (i.e. AM222, 67-3, and 305E40 versus AM22). The greatest differential expression among the genotypes was observed in the GO category 'biological processes' (BP), including the subcategories 'response to inorganic substances', 'response to abiotic stimulus', and 'cellular response to nitrogen starvation' (GO:0006995; Supplementary Table S4). Considering only the BP terms that were significantly over-represented ($P<0.05$), we were able to identify a number of DEGs shared by the N-use efficient genotypes (AM222 and 67-3) when compared to AM22, the most inefficient one (Fig. 2).

Identification of responsive genes by GO subcategories in roots and shoots

In roots at T0 (i.e. before the start of the N supply), the genotypes AM222, 67-3, and 305E40 shared 18 DEGs compared with AM22 in the category 'response to inorganic substances', five of which appeared to be involved in N uptake and metabolism. In addition, AM222 and 67-3 shared 14 DEGs, which included a stress-response gene in the form of a chaperonine heat-shock protein and a high-affinity nitrate transporter-like (Supplementary Table S5A).

At T1, after 24 h of N supply, AM222 and 67-3 shared 14 DEGs in the root transcriptome compared with AM22, some of which were related to multiple-stress responses, such as another chaperonine heat-shock protein, a plastid-lipid-associated chloroplastic-like, and a catalase (CAT) in the subcategory 'response to inorganic substances'. Interestingly, among 20 DEGs found exclusively in AM222, an aquaporin pip2-7-like, a sucrose synthase, a cellulose synthase DNA-binding isoform 1, and a NADH-dependent glutamate synthase protein were up-regulated. Among 48 genes found exclusively in the comparison between 67-3 and AM22, many appeared to be related to plant stress responses (Supplementary Table S5B).

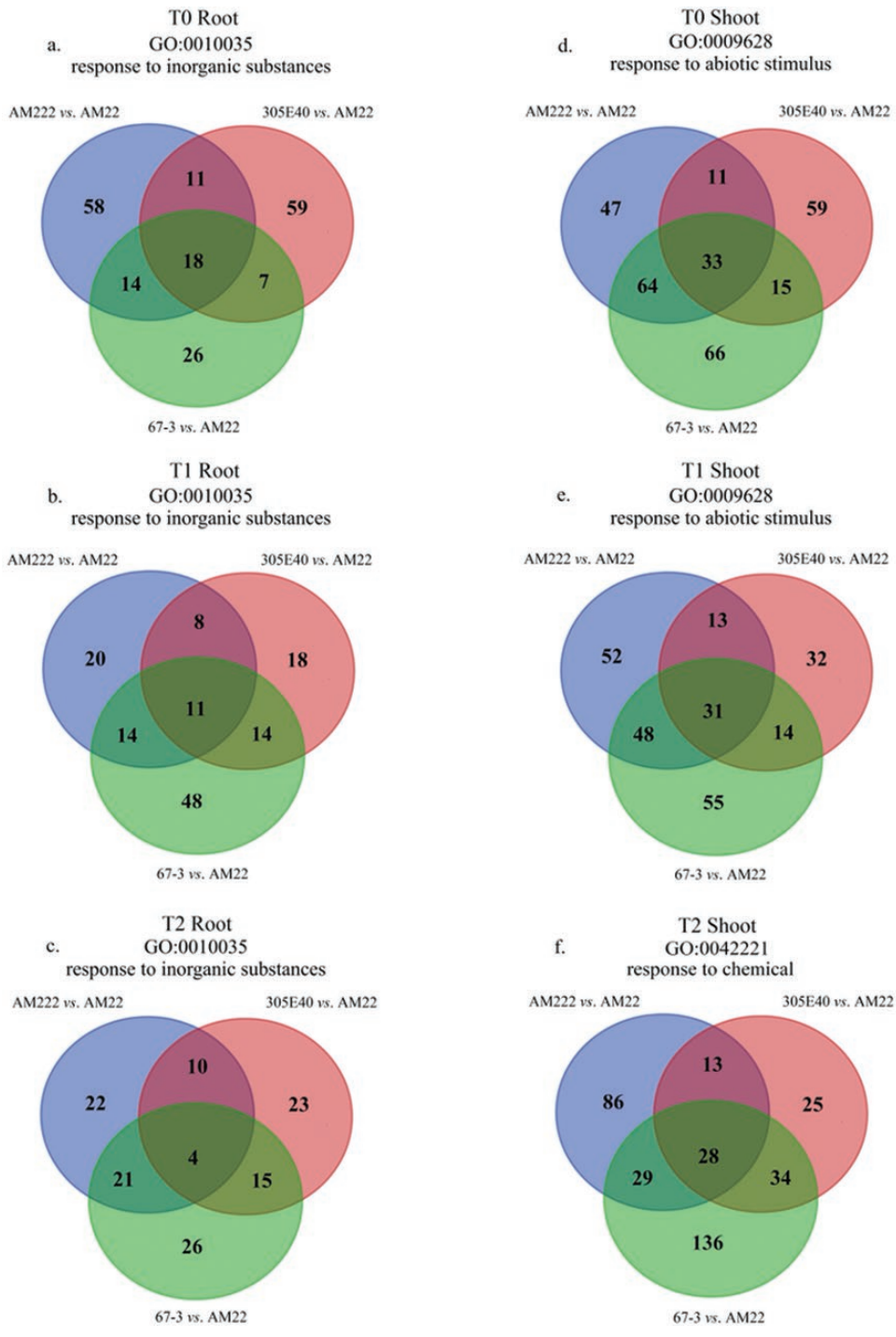

Fig. 2. Venn diagrams for Gene Ontology terms in eggplant genotypes that were significantly over-represented (P<0. 05) in comparisons with the low-NUE genotype AM22. Following N deprivation for 2 d, seedlings at 12 d old were supplied with 0.5 mM $Ca(NO_3)_2$. Samples were taken immediately prior to the N treatment (T0), after 24 h of treatment (T1), and after 16 d treatment (T2). (A–C) Shoots and (D–F) roots. Under low-N conditions, AM222 has the greatest NUE, followed by 67-3 and 305E40, with AM22 having the lowest NUE (Supplementary Fig. S1).

At T2, after 16 d of N supply, four DEGs in the roots belonging to 'response to inorganic substances' were shared with AM22 by all the other genotypes, while 21 DEGs were detected in the comparisons between AM222 and 67-3 with AM22. Notably, among these we identified a putative 33-like isoform of the WRKY transcription factor (WRKY33) (Fig. 2C, Supplementary Table S5A), a zinc-finger protein *ZAT10-like*, together with several genes related to calcium binding, and

genes responsive to drought and dehydration (Supplementary Table S5C).

In shoots at T0, the GO subcategory 'response to abiotic stimulus' was differentially modulated in AM222 and 67-3 compared with AM22, whereas no such effect was seen in 305E40. In particular, 64 genes were shared between AM222 and 67-3, among which were a nitrate reductase orthologue, a ferredoxin–NADP reductase (FNR), a zinc-finger protein *ZAT10*-like, and a light-harvesting chlorophyll *a–b* binding protein (LHCB; Supplementary Table S5D). Interestingly, at T_1, a significant number of DEGs in 'response to abiotic stimulus' were shared by AM222, 67-3, and 305E40 compared to AM22. Among these, LHCBs were identified (Supplementary Table S5E).

At T2, 21 DEGs in the category 'response to chemical' (GO:0042221) were up-regulated in the more N-use efficient genotypes, AM222 and 67-3, including two genes encoding proteins putatively involved in N nutrition, namely CAT and the ferredoxin–chloroplastic-like (Supplementary Table S5F). Overall, at T0 in the roots, AM222 and 67-3 shared a high-affinity nitrate transporter-like that was differentially regulated compared to the N-use inefficient genotype AM22. At T1, an aquaporin pip2-7-like and a NADH-dependent glutamate synthase protein were identified and, interestingly, at T2 *WRKY33* was strongly up-regulated in AM222 and 67-3 (Supplementary Table S6A). In the shoots at both T0 and T1, AM222 and 67-3 showed a strong up-regulation of a LHCB, and at T2 a ferredoxin–NADP reductase (FNR) and a catalase (CAT) were up-regulated (Supplementary Table S6B–D).

Gene co-expression networks

A comparative gene co-expression network construction and visualization (CoExpNetViz) approach was adopted to define independent gene co-expression networks (GCNs) based on selected 'bait genes'. Genes encoding four putative *LHCBs* (SMEL_003g193060.1, SMEL_005g230550.1, SMEL_008g310950.1, SMEL_008g308340.1), a *FNR* (SMEL_002g153410.1), a putative *CAT* (SMEL_005g238230.1), and a putative *WRKY33* orthologue (SMEL_006g257490.1) were employed.

Starting from the count read matrices, four independent GCNs were defined (Fig. 3). The network derived from the *LHCB*s included a cluster of 53 genes correlated with all four of the baits, while other genes were correlated with fewer (Fig. 3A, Supplementary Table S7A). Several other *LHCB*s and a PSI chloroplastic-like gene also appeared to be strongly correlated. The GCN obtained by using *FNR* as the bait showed four highly correlated genes (Fig. 3B, Supplementary Table S7B). Interestingly, a gene member of the auxin-responsive family (ARF) was highly co-expressed (Pearson correlation coefficient, PCC, 0.80202). The GCN obtained by using *CAT* as the bait showed 13 negatively correlated genes with lower absolute PCC values ranging from –0.61 to –0.65 (Fig. 3C, Supplementary Table S7C). Finally, the GCN obtained by using the putative *WRKY33* as bait showed 62 co-expressed genes, 21 of which had a PCC value >0.8 (Fig. 3D, Supplementary Table S7D). These included a zinc-finger DNA binding protein, a mitogen-activated protein kinase 3 (*MAPK3*), an auxin-responsive family gene (*ARF*), a stress-induced protein, and an ethylene-responsive 5-like gene (*ERF5*).

Correlations between gene networks and phenotypic data

We carried out a correlation analysis between the abundance of 85 gene transcripts (represented by the baits and those included in the GCN) and 32 morpho-physiological traits recently reported by Mauceri *et al.* (2020). Interestingly, we found that many genes from the *LHC*, *FNR*, *CAT*, and *WRKY33* networks were significantly correlated with biomass production, some root traits, and plant N and C contents, underlining their role in N-use and photosynthetic efficiencies (Supplementary Fig. S3, Supplementary Table S8).

RNA-seq data validation by RT-qPCR

Ten genes that showed relatively high expression ($P<0.05$) were selected from RNA-seq experiment for validation by qRT-PCR. These were the seven bait genes used for the GCN analysis (four *LHCB*s plus *FNR*, *CAT*, and *WRKY33*) together with three genes of interest from the *WRKY33* GCN (*Stress-induced protein*, *zinc-finger DNA-binding protein*, and *auxin-responsive familygene*). Statistical analysis of data for each genotype were reported in. Overall, Pearson correlation analysis between the RNA-seq and qRT-PCR experiments indicated a significant correlation ($r=0.813$; Supplementary Table S9A, Supplementary Fig. S4A).

To further validate the plant responses to low N, an independent experiment was carried out. At low-N supply, qRT-PCR analysis of five genes (*FNR*, *CAT*, *WRKY33*, *ZAT10*, *ARF*) confirmed that there was significantly different expression ($P<0.05$) between the N-use efficient and inefficient genotypes at T2 (Fig. 4, Supplementary Table S9B). *WRKY33* and other two genes from its co-network (*zinc-finger DNA-binding protein* and *auxin-responsive family*) shared the same expression profiles. Pearson correlation analysis between the RNA-seq and qRT-PCR data confirmed that there was a high and significant correlation ($r=0.839$; Supplementary Fig. S4B).

Root traits and NUE of AtWRKY33 transgenic lines

Phylogenetic analysis among eggplant *SmWRKY33*, tomato *SlWRKY33*, and all the WRKY family members from the Arabidopsis genome indicated that the highest similarity between both the Solanaceae sequences was with *AtWRKY33* (Supplementary Fig. S5A). In addition, we used the MEME tool to examine the structural organization of *WRKY33* from

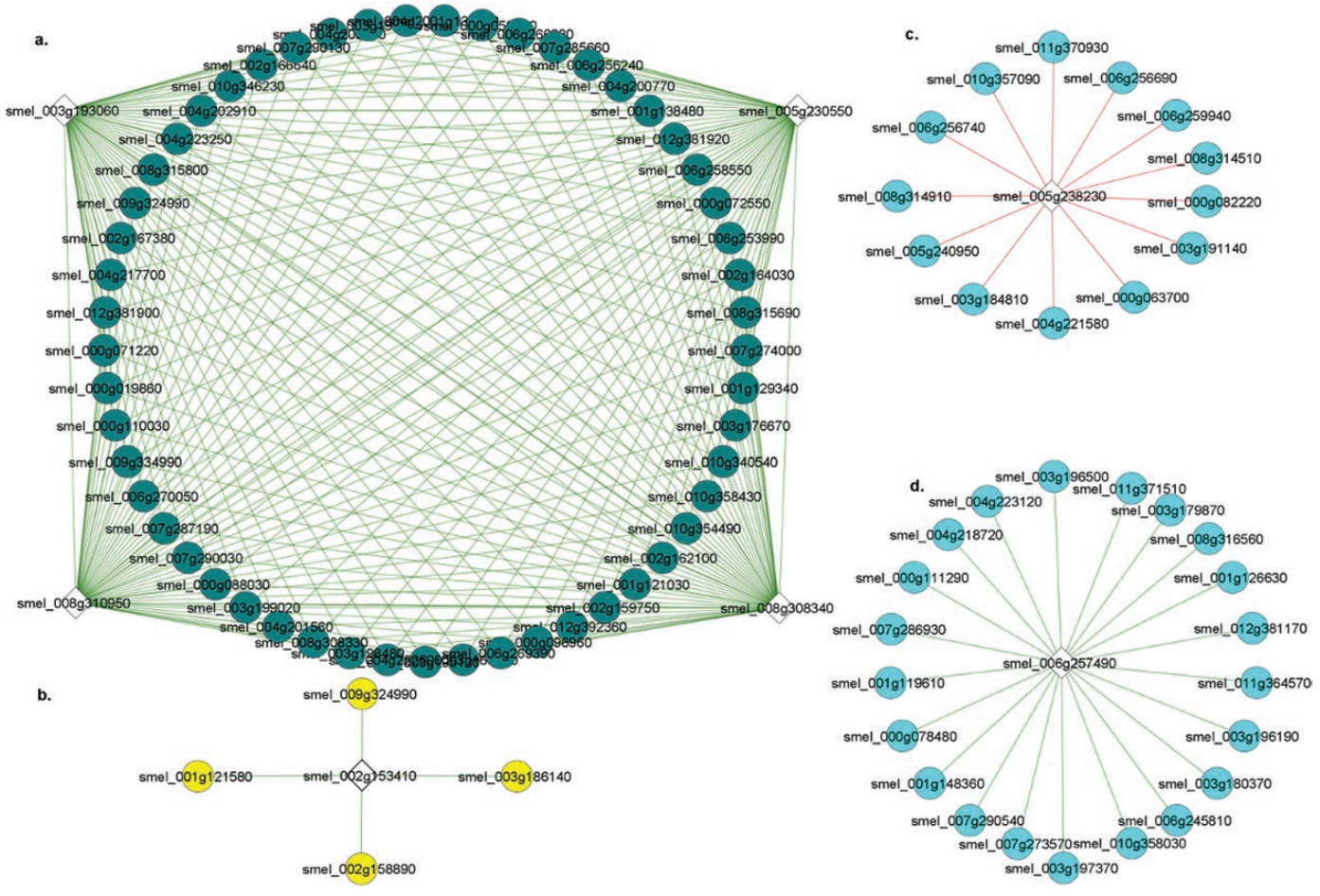

Fig. 3. Independent gene co-expression networks identified in four genotypes of eggplant with differing nitrogen-use efficiency subject to low N supply. The networks were obtained by using the following as bait: (A) four putative *LHCB* genes, (B) *ferredoxin–NADP reductase* (*FNR*), (C) catalase (*CAT*), and (D) a putative *WRKY33* orthologue (*WRKY33*). The baits are presented by diamonds, and positive and negative correlations are represented by green and red lines, respectively.

eggplant and Arabidopsis was also analyzed through MEME tool, and this identified conserved domains (Supplementary Fig. S5B).

The Arabidopsis Col-0 wild-type (WT), *wrky33-2*-knockout (KO) mutant, and *35S::AtWRKY33* overexpression (OE) transgenic line used for this experiment were first evaluated for *WRKY33* expression using RT-qPCR, which confirmed the lack of expression in the KO mutant and the overexpression in the OE line (Supplementary Table S9C).

The responses to low (0.5 mM) and high (10 mM) N supply showed that compared to the WT at low-N, the *35S:WRKY33* line exhibited significantly ($P<0.05$) higher values for total root length (95%), primary root length (14%), lateral root length (293%), and lateral root number (84%LRN). By contrast, differences in root morphology were not observed between the WT and the KO mutant. Interestingly, the differences were less marked at high N (Fig. 5A–D). The NUE values showed significant differences among genotypes (Fig. 5E). In particular, the OE transgenic line showed a higher NUE compared to the control at low N, whereas by contrast the WT showed a significantly higher NUE compared to the OE line at high N.

Discussion

The massive use of N-fertilizers to maximize crop yield is recognized as a costly and environmentally damaging practice (Ding *et al.*, 2015). Hence, reducing N input and breeding crops for higher nitrogen-use efficiency (NUE) are among the main goals in plant nutrition research (Hirel *et al.*, 2007) for a more sustainable agriculture (Masclaux-Daubresse *et al.*, 2010). In an effort to understand the mechanisms underlying NUE, many molecular and physiological approaches have been used across various species through omic techniques (Xu *et al.*, 2012). Among these, transcriptomics allows the dissection of N-dependent gene networks by looking at changes in transcript levels, including those of transcription factors (TFs; Fukushima and Kusano, 2014), especially when studies are carried out on genotypes with contrasting NUE (Zamboni *et al.*,

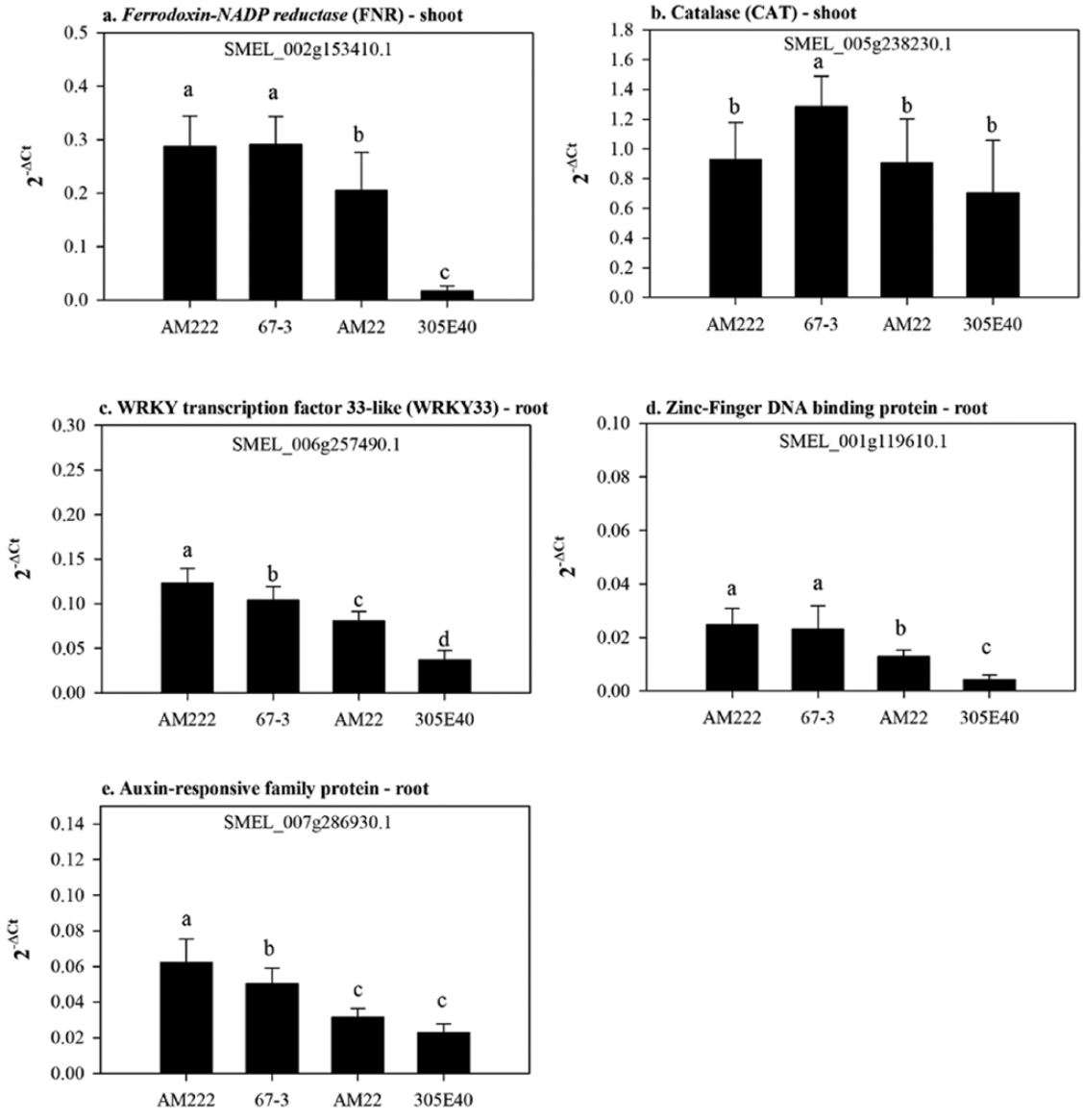

Fig. 4. Validation of RNA-seq results by quantitative real-time PCR (qRT-PCR) analysis for four genotypes of eggplant with differing nitrogen-use efficiency (NUE) subject to low N supply (0.5 mM). (A) *Ferredoxin–NADP reductase* (*FNR*) in shoots, (B) *catalase* (*CAT*) in shoots, (C) putative *WRKY33* orthologue (*WRKY33*) in roots, (D) *zinc-finger DNA-binding protein* in roots, and (E) *auxin-responsive family protein* in roots. Under low-N conditions, AM222 has the greatest NUE, followed by 67-3 and 305E40, with AM22 having the lowest NUE (Supplementary Fig. S1). Data are means (±SE) of n=5 replicates. Different letters indicate significant differences between means as determined using Fisher's LSD method (P<0.05).

2014). In our study, we used transcriptomic analysis to identify key genes in response to short- and long-term nitrogen limitation in eggplant (aubergine, *Solanum melongena*) genotypes with contrasting NUE (Mauceri *et al.*, 2020).

PCA and differentially expressed genes

In order to evaluate the gene expression profiles of four genotypes known to have different responses to limited N availability, a principle component analysis (PCA) was carried out, which clearly separated the N-use efficient and inefficient genotypes, mainly after short-term exposure to low N (Fig. 1). These observations were confirmed by the detection of a high number of differentially expressed genes (DEGs) among the genotypes in both the shoots and roots, at all the sampling times (Supplementary Table S2). Many DEGs have previously been identified in low-N tolerant and sensitive barley genotypes under N stress, including genes for N-transporters, TFs, kinases, and genes related to antioxidant stress and hormone signaling (Quan *et al.*, 2016). Such studies have allowed clarification of the complex plant nitrate regulatory network at the transcriptional level, and the development of pipelines for

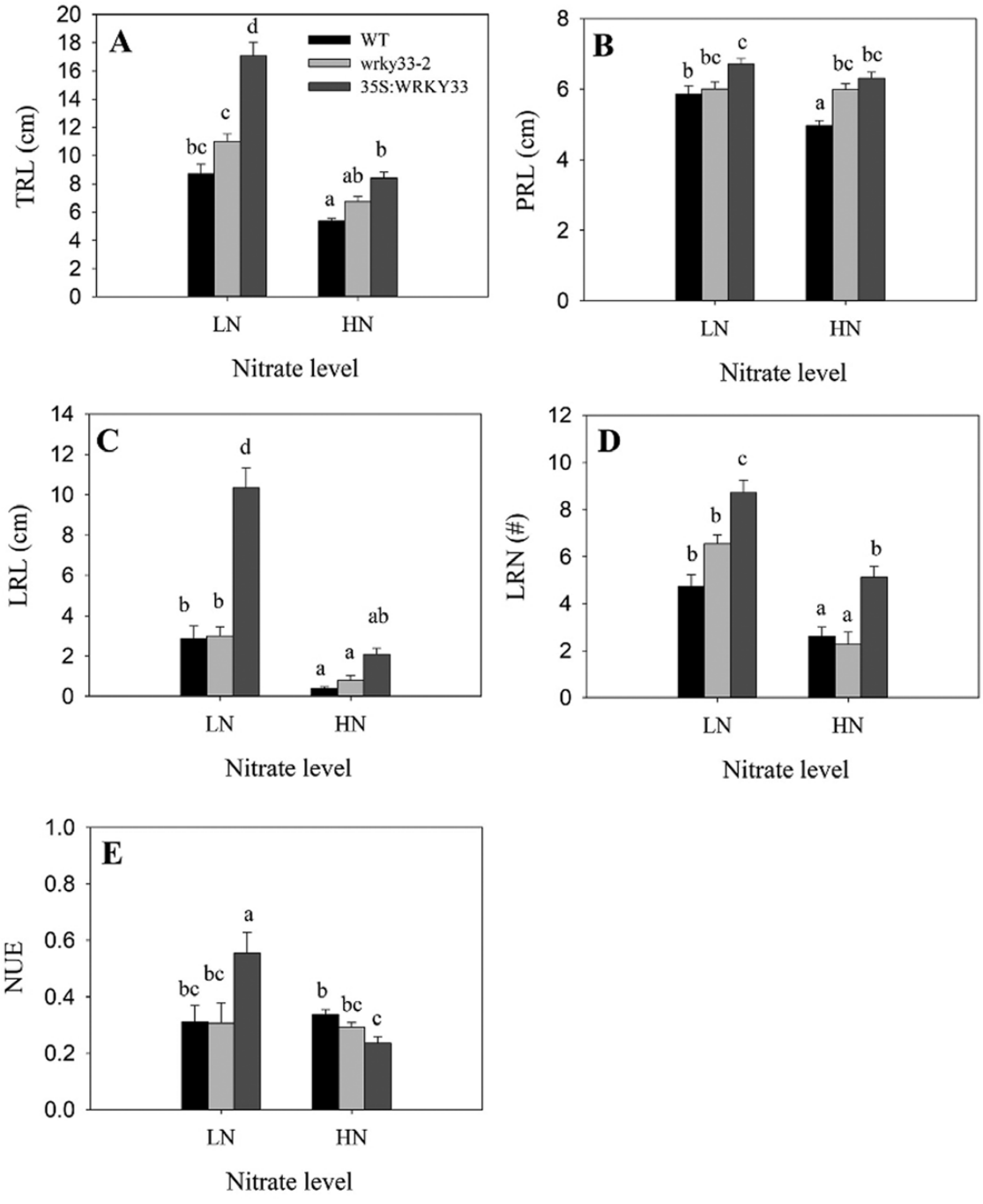

Fig. 5. Root morphology and nitrogen use efficiency in Arabidopsis Col-0 wild-type (WT) plants, the *wrky33-2* knockout mutant, and a transgenic *35S::AtWRKY33* overexpression line exposed to either low nitrate (LN, 0.5 mM) or high nitrate (HN, 10 mM) for 7 d. (A) Total root length (TRL), (B) primary root length (PRL), (C) lateral root length (LRL), (D) lateral root number (LRN), and (E) nitrogen use efficiency (NUE). The values represent the mean ± error standard. Data are means (±SE) of n=18 replicates. Different letters indicate significant differences as determined using ANOVA followed by Tukey's test (P<0.05).

analysing large biological datasets through network analysis has become a key approach (Tzfadia *et al.*, 2016).

Using MapMan metabolic pathways analysis, we observed a different pattern of gene expression linked to light reactions between the more N-use efficient genotypes,AM222 and 67-3, and the inefficient ones, AM22 and 305E40 (Supplementary Fig. S2). In particular, the light-harvesting complexes (LHCs, localized generally in the chloroplast thylakoid membrane) and the ferredoxin–NADP reductase (FNR) appeared as the most notable gene clusters involved in NUE. Interestingly, our

results from a previous study showed that the N-use efficiency of AM222 and 67-3 was mainly determined by the nitrogen utilization efficiency (NUtE) component (Mauceri *et al.*, 2020). This suggests that the higher uptake of N primarily supports photosynthesis, as evidenced by the up-regulation of LHC genes in AM222 and 67-3 compared to AM22 (the most inefficient genotype). Consistent with this, it has been reported that a greater allocation of Rubisco is made towards the LHCs at low light and for a given N availability in order to maximize light capture (Kumar *et al.*, 2002). LHC complexes are involved in the transduction of energy for photosynthesis and also in the production of reactive oxygen species (ROS) production, confirming their key role in photosynthesis (Tanaka *et al.*, 2001; Klimmek *et al.*, 2006).

The significant up-regulation of *FNR* observed in the N-use efficient genotypes at T2 (16 d of N supply; Fig. 4) was of interest because of the role of the FNR protein in mediating the transfer of electrons in the chloroplast from reduced ferredoxin (Fd) to $NADP^+$ (generating NADPH), which is required for carbon assimilation (Mulo, 2011). This protein is also involved in the re-assimilation of ammonia released during photorespiration via Fd-GOGAT and in the maintenance of optimal redox balance in plastids (Foyer *et al.*, 2009; Eisenhut *et al*, 2019). The FNR protein is also involved in ROS quenching to preserve $NADP^+$/NADPH homeostasis and to avoid oxidative stress (Palatnik *et al.*, 1997, 2003). Furthermore, nitrite generated in the cytosol is imported into the chloroplasts and reduced to ammonium by FD-dependent NiR in order to sustain high NUE (Hoff *et al.*, 1994; Sugiura *et al.*, 2007). Therefore, we may assume that up-regulation of FNR in eggplant also contributes to NUE by lowering energy costs in both the nitrate assimilation and oxidative stress responses, as previously reported by Hanke *et al.* (2005) and Lintala *et al.* (2007).

GO enrichment analysis

GO enrichment analysis among the genotypes revealed five genes involved in 'response to nitrate' (GO: 0010167), including genes belonging to the NRT1/PTR FAMILY 6.3-like (Table 1). These genes were significantly up-regulated in the roots of the efficient genotypes, particularly in AM222. NPF6.3/NRT1.1 is a dual-affinity NO_3^- transporter that is able to transport auxin (Krouk *et al.*, 2010; Gojon *et al.*, 2011), and a NO_3^--sensing function as well as NO_3^--induced changes in root development have also been reported (Huang *et al.*, 1999; Remans *et al.*, 2006). Therefore, higher gene expression of the NRT1/PTR family in the N-use efficient root genotypes could support their role in NO_3^- uptake and root development. The other DEGs included a *CLC-B* for N storage into the vacuole, *BTB1*, which acts as a mediator for multiple responses to nutrients, stress, and auxins (Mandadi *et al.*, 2009; Robert *et al.*, 2009), and the *NIR1*, which encodes a key enzyme involved in the reduction of ammonium nitrite. These results could therefore explain the relatively high NUE of AM222 at low N compared to the other genotypes, enabling it to take up and accumulate higher amounts of N into its tissues.

Our GO enrichment analysis among the genotypes, which identified changes in subcategories including 'response to inorganic substances' (GO:0010035), 'response to abiotic stimulus' (GO:0009628), and 'cellular response to nitrogen starvation' (GO:0006995), allowed us to identify other modulated genes shared by the more N-use efficient genotypes, in both the roots and shoots (Supplementary Table S4). Specifically, a higher expression of catalase (CAT, the enzyme involved in protection against H_2O_2) was evident in the shoots of both the N-use efficient genotypes. H_2O_2 is a well-known toxic ROS molecular species, mainly produced during photosynthesis and photorespiration, that is able to cause damage to cellular structures and also performs a signaling molecule in transduction networks for abiotic stimuli (Xing *et al.*, 2008; Li *et al.*, 2015).

Following long-term low-N stress (16 d), we identified highly significant up-regulation of *WRKY33* in the N-use efficient root genotypes (Fig. 4). Several TFs have been described that are capable of modulating plant responses to N limitation, and the WRKY family plays a multitude of roles in plants, for example regulating normal growth and development as well as responses to different stimuli (Jiang *et al.*, 2017), and being able to confer tolerance to some biotic and abiotic stresses, including H_2O_2 production (Jiang and Yu, 2009; Song *et al.*, 2009). Interestingly, the TF WRKY1 has been reported to be involved in the genome-wide transcriptional reprogramming of Arabidopsis exposed to light and N stress both individually and in combination (Heerah *et al.*, 2019).

Gene co-expression network analysis reveals gene clusters related to NUE

Using *LHCB*s as baits, our co-expression network analysis identified a variety of genes involved in photosynthesis, light-harvesting, porphyrin formation, and tetrapyrrole biosynthetic processes (Fig. 3A). In particular, the glyceraldehyde-3-phosphate dehydrogenase chloroplastic-like gene (*GAPCP*) was up-regulated in the N-use efficient genotypes; it encodes a key enzyme for starch breakdown to form sucrose and to generate primary metabolites employed for the synthesis of fatty acids and amino acids (Muñoz-Bertomeu *et al.*, 2009).

Auxin-responsive family gene was also found in the same network (Fig. 3A), the physiological functions of which included the utilization of ascorbate as an electron donor, which provides energy for trans-membrane transport. These processes result in plant defense against stress and in cell wall modifications (Asard *et al.*, 2013). In addition, the high expression of the protochlorophyllide chloroplastic-like and coproporphyrinogen-III chloroplastic-like genes, which encode for proteins involved in tetrapyrrole biosynthesis (Kobayashi and Masuda, 2016), suggested that the N-use

efficient genotypes might produce chlorophyll more efficiently than the inefficient ones.

In the *FNR* gene co-expression network, another auxin-responsive family gene member and a fructose-bisphosphate aldolase chloroplastic-like (FBA) were identified (Fig. 3B). FNR is the main source of electrons whose distribution is essential for metabolic reactions, for biosynthesis of chlorophyll and fatty acids, and assimilation of CO_2, nitrogen, and sulphur (Hanke *et al.*, 2005; Hanke and Mulo, 2013). Therefore, higher expression of these genes under limited N supply might increase the photosynthetic capacity of AM222 and 67-3, contributing to their higher NUE. In addition, the FBA enzyme family plays key roles in glycolysis, gluconeogenesis, and in the Calvin cycle, suggesting that differences in gene expression will result in different responses to abiotic stress and in plant development, as previously reported (Lu *et al.*, 2012; Lv *et al.*, 2017). Thus, higher *FBA* expression in the N-use efficient genotypes might positively influence the turnover of the Calvin cycle and hence improve the photosynthetic rate (Uematsu *et al.*, 2012).

Using *WRKY33* as bait, our co-expression network analysis indicated that concurrent higher expression of other TFs and genes correlated with the stress responses (Fig. 3D). Interestingly, the more abundant transcripts in this network belonged the mitogen-activated protein kinase (*MAPK*) family, together with *yellow-leaf-specific 9* (*YLS9*), a zinc-finger protein ZAT10-like, and two ethylene-responsive TFs like (ERFs). In plants, *MAPK*s play important roles in several signaling networks involved in plant responses to environment; interestingly, up-regulation of a MAP kinase in response to nutritional deficiency and N-signaling has recently been reported (Chardin *et al.*, 2017). Furthermore, a role for *YLS9* in N remobilization and recycling that is useful for plant adaptation and survival in unfavorable environmental conditions has also been reported (Yoshida *et al.*, 2001). Thus, up-regulation of *YLS9* suggests that the N-use efficient genotypes have higher N remobilization compared to the inefficient genotypes.

Plant stress responses and related signal transduction pathways are also controlled by the *ERF*TF family. *ERF5* and *ERF6* have been reported to activate other stress-related TFs such as WRKY33 and MYB51 under water stress in Arabidopsis, and the zinc-finger protein ZAT10, which modulates abiotic stress responses and reactive oxygen-defense (Mittler *et al.*, 2006; Dubois *et al.*, 2013). In the *WRKY33* network, both *ERF4* and *ERF5* together with a ZAT10-like protein were consistently up-regulated in AM222 (Fig. 3D).

In order to decipher the complexity of the responses of the different eggplant genotypes under N-stress, we examined Pearson's correlation coefficients between phenotypic traits and gene expression. Significant correlations were found between the DEGs that we identified and many phenotypic and physiological traits previously reported by Mauceri *et al.* (2020) (Supplementary Fig. S3). These included both the components of NUE, shoot dry weight (plant biomass), root and shoot C and N contents, together with many root traits, among which the total root length appeared the most interesting. We found that high N contents in the roots and shoots in the N-use efficient compared to the inefficient genotypes correlated with higher differential expression of *LHC*s, *auxin-responsive family gene*, *FNR*, *CAT*, *WRKY33*, and *ZAT10*, making them of considerable interest to explain the differences in NUE. The array of DEGs that we have identified have the potential to deepen our understanding of the molecular mechanisms associated with responses to N limitation and other environmental stresses.).

Expression of NUE-related genes in eggplant and in a transgenic Arabidopsis WRKY-*overexpression line*

We validated the RNA-seq data through expression analysis of the seven bait genes used in the gene co-expression networks together with three other genes of interest included in the *WRKY33* cluster that showed higher transcript abundance in the high-NUE genotypes, namely those encoding Stress-induced protein, Zinc-finger DNA-binding protein, and Auxin-responsive family protein.

To help confirm the biological significance of our results, we used a hydroponic experiment to examine the expression patterns of five of the key genes that we had identified in the responses of the different genotypes to low N, namely those encoding FNR, CAT, WRKY33, ZAT10, and auxin-responsive family protein (Fig. 4). In shoots, *FNR* was up-regulated in the more N-use efficient genotypes AM222 and 67-3 compared with the inefficient ones, AM22 and 305E40. In the roots, significant up-regulation of *WRKY33* under low N was observed in AM222 and 67-3, suggesting its involvement in the greater N-use efficiency in these genotypes. *Stress-induced protein*, *Zinc-finger DNA-binding protein*, and *Auxin-responsive family protein* also showed the same expression pattern at low N supply between the efficient and inefficient genotypes.

We also examined an Arabidopsis *35S::AtWRKY33* overexpression transgenic line and found that in comparison to the wild-type it displayed phenotypic traits that were significantly correlated to an improved response to low N caused by a modulation of the *WRKY33* co-network genes (Fig. 5). The overexpression line was characterized by a greater number and increased length of lateral roots, as previously observed in AM222 (Mauceri *et al.*, 2020). Correlations between quantitative trait loci for N-uptake and root traits can aid selection for root systems that take up N more efficiently and hence improve NUE and crop yield (Coque *et al.* 2008). Increased length and a greater number of lateral roots allows more efficient soil exploration and nutrient acquisition with consequent higher crop yields (Postma *et al.*, 2014).

Conclusions

Our comparison using transcriptomics of eggplant genotypes with contrasting NUE showed regulation by coordinated gene networks in order to cope with limited N availability. We identified several DEGs between N-use efficient and inefficient genotypes that were useful in understanding the molecular mechanisms for increasing NUE. Genes related to the light-harvesting complexes (LHCs) and ferredoxin–NADP reductase (FNR) involved in the light reaction pathway were up-regulated in the N-use efficient genotypes, confirming the key role of photosynthetic efficiency for increasing NUE in response to low N in eggplant. Our GO results also highlighted the role of genes involved in responses to inorganic substances, abiotic stimuli, and chemicals. Among these, we identified the WRKY33 transcription factor, the co-expression network of which at low N supply included up-regulation of *MAP* kinases and *YLS9*, indicating that the high sensitivity to N and the remobilization are key processes in the N-use efficient genotypes. *WRKY33* also triggered up-regulation of an *auxin-responsive family gene*, which may promote the development of a root system that can capture N more efficiently from the soil, as confirmed by the transgenic Arabidopsis *AtWRKY33* line overexpressing the closest orthologue for *SmWRKY33*. Thus, an efficient photosynthetic apparatus, a competitive root system, and active N-remobilization appear to be the key processes that confer high NUE in eggplants.

Supplementary data

The following supplementary data are available at *JXB* online.

Table S1. List of primer used in this study.

Table S2. Differentially expressed genes between pairs of genotypes at each time-point and in each tissue.

Table S3. GO enrichment for each genotype in roots and shoots at T1 versus T0.

Table S4. GO enrichment between AM22 and the other three genotypes.

Table S5. The GO terms significantly over-represented that were useful in highlighting the differentially expressed genes in all possible logical relationships.

Table S6. Differential expression analysis of *WRKY33-like*, *Light-harvesting complex*, *Ferredoxin–NADP reductase*, and *catalase*.

Table S7. Genes involved in the coordinated gene networks obtained by using *LHCB*s, *FNR*, *WRKY33*, and *CAT* as bait.

Table S8. Significant correlations among gene expression obtained in this study and morphophysiological traits reported by Mauceri *et al.* (2020).

Table S9. Mean values for $2^{\Delta\Delta CT}$ values in the qRT-PCR experiments.

Fig. S1. Nitrogen use efficiency, N-utilization efficiency, and N-uptake efficiency of the different eggplant genotypes.

Fig. S2. Overview of differences in transcripts abundance related to primary and secondary metabolism pathways in comparisons between genotypes, time-points, and tissues.

Fig. S3. Significant correlations among gene expression obtained in this study and morphophysiological traits reported by Mauceri *et al.* (2020).

Fig. S4. Pearson correlations between RNA-seq normalized read counts and RT-qPCR relative quantification data.

Fig. S5. Phylogenetic tree of Arabidopsis *WRKY*, eggplant and tomato homologous peptide sequences, and sequence motifs of related WRKY33 and Arabidopsis protein sequences.

Acknowledgements

We would like to thank Alberto Pallavicini, Marco Gerdol, and Samuele Greco from the Dipartimento di Scienze della Vita at the Università degli Studi di Trieste for their technical assistance in the bioinformatics analysis; Efrat Almekias-Siegl from the Department of Plant and Environmental Sciences, Weizmann Institute of Science, Rehovot – Israel; and Prof. S. AbuQamar, Department of Biology, United Arab Emirates University for kindly providing the Arabidopsis *AtWRKY33* transgenic line. This project was supported by SOLNUE ('Tomato and eggplant nitrogen utilization efficiency in Mediterranean environments') in the framework H2020 SusCrop-ERA-NET ID#47. We also thank the CNR project FOE-2019 DBA.AD003.139 for supporting the research activity of FM. The authors declare that they have no conflicts of interest in relation to this work.

Author contributions

AM, MRA, FS, GLR, and AL planned the experiments; SP prepared the TranSeq libraries; AM, MMA, and AL carried out the hydroponic experiments and extracted the RNA; AM, LT, FM, FS, and AL analysed the data; MMA, and AL carried out the Arabidopsis experiments; AM, MRA, LT, FM, AA, FS, GLR, and AL were involved in drafting the paper; all the authors read and approved the final version of the paper.

Data availability

The RNA-seq data used in this study is available at the NCBI Sequence Read Achieve (http://www.ncbi.nlm.nih.gov/sra) with the accession number PRJNA643937.

References

Abenavoli MR, Longo C, Lupini A, Miller AJ, Araniti F, Mercati F, Princi MP, Sunseri F. 2016. Phenotyping two tomato genotypes with different nitrogen use efficiency. Plant Physiology and Biochemistry **107**, 21–32.

Abenavoli MR, Nicolò A, Lupini A, Oliva S, Sorgonà A. 2008. Effects of different allelochemicals on root morphology of *Arabidopsis thaliana*. Allelopathy Journal **22**, 245–252.

Amiour N, Imbaud S, Clément G, Agier N, Zivy M, Valot B, Balliau T, Armengaud P, Quilleré I, Cañas R. 2012. The use of metabolomics integrated with transcriptomic and proteomic studies for identifying key steps

involved in the control of nitrogen metabolism in crops such as maize. Journal of Experimental Botany **63**, 5017–5033.

Anders S, Pyl PT, Huber W. 2015. HTSeq—a Python framework to work with high-throughput sequencing data. Bioinformatics **31**, 166–169.

Ansorge WJ. 2009. Next-generation DNA sequencing techniques. Nature Biotechnology **25**, 195–203.

Asard H, Barbaro R, Trost P, Bérczi A. 2013. Cytochromes *b*561: ascorbate-mediated trans-membrane electron transport. Antioxidants & Redox Signaling **19**, 1026–1035.

Bailey TL, Boden M, Buske FA, Frith M, Grant CE, Clementi L, Ren J, Li WW, Noble WS. 2009. MEME Suite: tools for motif discovery and searching. Nucleic Acids Research **37**, W202–W208.

Banerjee A, Roychoudhury A. 2015. WRKY proteins: signaling and regulation of expression during abiotic stress responses. The Scientific World Journal **2015**, 807560.

Barbierato V, Sala T, Rinaldi P, Bassolino L, Barchi L, Rotino GL, Toppino L. 2017. A spiking strategy facilitates housekeeping selection for RT-qPCR analysis under different biotic stresses in eggplant. Protoplasma **254**, 2215–2223.

Barchi L, Pietrella M, Venturini L, *et al.* 2019. A chromosome-anchored eggplant genome sequence reveals key events in Solanaceae evolution. Scientific Reports **9**, 11769.

Benjamini Y, Hochberg Y. 1995. Controlling the false discovery rate: a practical and powerful approach to multiple testing. Journal of the Royal Statistical Society: Series B **57**, 289–300.

Cericola F, Portis E, Toppino L, Barchi L, Acciarri N, Ciriaci T, Sala T, Rotino GL, Lanteri S. 2013. The population structure and diversity of eggplant from Asia and the Mediterranean Basin. PLoS ONE **8**, e73702.

Chardin C, Schenk ST, Hirt H, Colcombet J, Krapp A. 2017. Mitogen-activated protein kinases in nutritional signaling in Arabidopsis. Plant Science **260**, 101–108.

Chardon F, Barthélémy J, Daniel-Vedele F, Masclaux-Daubresse C. 2010. Natural variation of nitrate uptake and nitrogen use efficiency in *Arabidopsis thaliana* cultivated with limiting and ample nitrogen supply. Journal of Experimental Botany **61**, 2293–2302.

Chardon F, Noël V, Masclaux-Daubresse C. 2012. Exploring NUE in crops and in Arabidopsis ideotypes to improve yield and seed quality. Journal of Experimental Botany **63**, 3401–3412.

Coque M, Martin A, Veyrieras J, Hirel B, Gallais A. 2008. Genetic variation for N-remobilization and postsilking N-uptake in a set of maize recombinant inbred lines. 3. QTL detection and coincidences. Theoretical and Applied Genetics **117**, 729–747.

Ding WX, Chen ZM, Yu HY, Luo JF, Yoo GY, Xiang J, Zhang HJ, Yuan JJ. 2015. Nitrous oxide emission and nitrogen use efficiency in response to nitrophosphate, N-(n-butyl) thiophosphoric triamide and dicyandiamide of a wheat cultivated soil under sub-humid monsoon conditions. Biogeosciences **12**, 803–815.

Dobin A, Davis CA, Schlesinger F, Drenkow J, Zaleski C, Jha S, Batut P, Chaisson M, Gingeras TR. 2013. STAR: ultrafast universal RNA-seq aligner. Bioinformatics **29**, 15–21.

Dubois M, Skirycz A, Claeys H, *et al.* 2013. ETHYLENE RESPONSE FACTOR6 acts as a central regulator of leaf growth under water-limiting conditions in Arabidopsis. Plant Physiology **162**, 319–332.

Eisenhut M, Roell MS, Weber APM. 2019. Mechanistic understanding of photorespiration paves the way to a new green revolution. New Phytologist **223**, 1762–1769.

Eulgem T, Rushton PJ, Robatzek S, Somssich IE. 2000. The WRKY superfamily of plant transcription factors. Trends in Plant Science **5**, 199–206.

Ferrante A, Nocito FF, Morgutti S, Sacchi GA. 2017. Plant breeding for improving nutrient uptake and utilization efficiency. In: Tei F, Nicola S, Benincasa P, eds. Advances in research on fertilization management of vegetable crops. Advances in olericulture. Cham, Switzerland: Springer.

Foyer CH, Bloom AJ, Queval G, Noctor G. 2009. Photorespiratory metabolism: genes, mutants, energetics, and redox signaling. Annual Review of Plant Biology **60**, 455–484.

Fukushima A, Kusano M. 2014. A network perspective on nitrogen metabolism from model to crop plants using integrated 'omics' approaches. Journal of Experimental Botany **65**, 5619–5630.

Gantasala NP, Papolu PK, Thakur PK, Kamaraju D, Sreevathsa R, Rao U. 2013. Selection and validation of reference genes for quantitative gene expression studies by real-time PCR in eggplant (*Solanum melongena* L). BMC Research Notes **6**, 312.

Garnett T, Conn V, Kaiser BN. 2009. Root based approaches to improving nitrogen use efficiency in plants. Plant, Cell & Environment **32**, 1272–1283.

Gelli M, Duo Y, Konda AR, Zhang C, Holding D, Dweikat I. 2014. Identification of differentially expressed genes between sorghum genotypes with contrasting nitrogen stress tolerance by genome-wide transcriptional profiling. BMC Genomics **15**, 179.

Gerst R, Hölzer M. 2019. PCAGO: an interactive web service to analyze RNA-seq data with principal component analysis. bioRxiv doi:10.1101/433078. [Preprint].

Gojon A, Krouk G, Perrine-Walker F, Laugier E. 2011. Nitrate transceptor(s) in plants. Journal of Experimental Botany **62**, 2299–2308.

Good AG, Shrawat AK, Muench DG. 2004. Can less yield more? Is reducing nutrient input into the environment compatible with maintaining crop production? Trends in Plant Science **9**, 597–605.

Greenwood DJ, Stone DA, Draycott A. 1990. Weather, nitrogen-supply and growth rate of field vegetables. Plant and Soil **124**, 297–301.

Hanke G, Mulo P. 2013. Plant type ferredoxins and ferredoxin-dependent metabolism. Plant, Cell & Environment **36**, 1071–1084.

Hanke GT, Okutani S, Satomi Y, Takao T, Suzuki A, Hase T. 2005. Multiple iso-proteins of FNR in Arabidopsis: evidence for different contributions to chloroplast function and nitrogen assimilation. Plant, Cell & Environment **28**, 1146–1157.

Hao QN, Zhou XA, Sha AH, Wang C, Zhou R, Chen SL. 2011. Identification of genes associated with nitrogen-use efficiency by genome-wide transcriptional analysis of two soybean genotypes. BMC Genomics **12**, 525.

Hawkesford MJ. 2012. The diversity of nitrogen use efficiency for wheat varieties and the potential for crop improvement. Better Crops **96**, 10–12.

He GH, Xu JY, Wang YX, Liu JM, Li PS, Chen M, Ma YZ, Xu ZS. 2016. Drought-responsive WRKY transcription factor genes *TaWRKY1* and *TaWRKY33* from wheat confer drought and/or heat resistance in Arabidopsis. BMC Plant Biology **16**, 116.

He X, Qu B, Li W, Zhao X, Teng W, Ma W, Ren Y, Li B, Li Z, Tong Y. 2015. The nitrate-inducible NAC transcription factor TaNAC2-5A controls nitrate response and increases wheat yield. Plant Physiology **169**, 1991–2005.

Heerah S, Katari M, Penjor R, Coruzzi G, Marshall-Colon A. 2019. WRKY1 mediates transcriptional regulation of light and nitrogen signaling pathways. Plant Physiology **181**, 1371–1388.

Hirakawa H, Shirasawa K, Miyatake K, *et al.* 2014. Draft genome sequence of eggplant (*Solanum melongena* L.): the representative *Solanum* species indigenous to the old world. DNA Research **21**, 649–660.

Hirel B, Le Gouis J, Ney B, Gallais A. 2007. The challenge of improving nitrogen use efficiency in crop plants: towards a more central role for genetic variability and quantitative genetics within integrated approaches. Journal of Experimental Botany **58**, 2369–2387.

Hoff T, Truong HN, Caboche M. 1994. The use of mutants and transgenic plants to study nitrate assimilation. Plant, Cell & Environment **17**, 489–506.

Huang NC, Liu KH, Lo HJ, Tsay YF. 1999. Cloning and functional characterization of an Arabidopsis nitrate transporter gene that encodes a constitutive component of low-affinity uptake. The Plant Cell **11**, 1381–1392.

Jiang J, Ma S, Ye N, Jiang M, Cao J, Zhang J. 2017. WRKY transcription factors in plant responses to stresses. Journal of Integrative Plant Biology **59**, 86–101.

Jiang WB, Yu DQ. 2009. Arabidopsis WRKY2 transcription factor may be involved in osmotic stress response. Acta Botanica Yunnanica **31**, 427–432.

Kant S, Bi YM, Rothstein SJ. 2011. Understanding plant response to nitrogen limitation for the improvement of crop nitrogen use efficiency. Journal of Experimental Botany **62**, 1499–1509.

Klimmek F, Sjödin A, Noutsos C, Leister D, Jansson S. 2006. Abundantly and rarely expressed *Lhc* protein genes exhibit distinct regulation patterns in plants. Plant Physiology **140**, 793–804.

Kobayashi K, Masuda T. 2016. Transcriptional regulation of tetrapyrrole biosynthesis in *Arabidopsis thaliana*. Frontiers in Plant Science **7**, 1811.

Krouk G, Lacombe B, Bielach A, *et al.* 2010. Nitrate-regulated auxin transport by NRT1.1 defines a mechanism for nutrient sensing in plants. Developmental Cell **18**, 927–937.

Kumar PA, Parry MAJ, Mitchell RAC, Ahmad A, Abrol YP. 2002. Photosynthesis and nitrogen-use efficiency. In Foyer CH, Noctor G, eds. Photosynthetic nitrogen assimilation and associated carbon and respiratory metabolism. Dordrecht: Springer Verlag Netherlands, 23–34.

Léran S, Garg B, Boursiac Y, Corratgé-Faillie C, Brachet C, Tillard P, Gojon A, Lacombe B. 2015. AtNPF5.5, a nitrate transporter affecting nitrogen accumulation in *Arabidopsis* embryo. Scientific Reports **5**, 7962.

Li J, Gao Z, Zhou L, Li L, Zhang J, Liu Y, Chen H. 2019. Comparative transcriptome analysis reveals K^+ transporter gene contributing to salt tolerance in eggplant. BMC Plant Biology **19**, 67.

Li J, He YJ, Zhou L, Liu Y, Jiang M, Ren L, Chen H. 2018. Transcriptome profiling of genes related to light-induced anthocyanin biosynthesis in eggplant (*Solanum melongena* L.) before purple color becomes evident. BMC Genomics **19**, 201.

Li J, Liu J, Wang G, *et al.* 2015. A chaperone function of NO CATALASE ACTIVITY1 is required to maintain catalase activity and for multiple stress responses in Arabidopsis. The Plant Cell **27**, 908–925.

Li S, Fu Q, Chen L, Huang W, Yu D. 2011. *Arabidopsis thaliana* WRKY25, WRKY26, and WRKY33 coordinate induction of plant thermotolerance. Planta **233**, 1237–1252.

Lintala M, Allahverdiyeva Y, Kidron H, Piippo M, Battchikova N, Suorsa M, Rintamaeki E, Salminen TA, Aro EM, Mulo P. 2007. Structural and functional characterization of ferredoxin-$NADP^+$-oxidoreductase using knock-out mutants of Arabidopsis. Plant Journal **49**, 1041–1052.

Livak KJ, Schmittgen TD. 2001. Analysis of relative gene expression data using real-time quantitative PCR and the $2^{-\Delta\Delta}C^T$ method. Methods **25**, 402–408.

Lo Scalzo R, Fibiani M, Francese G, D'Alessandro A, Rotino GL, Conte P, Mennella G. 2016. Cooking influence on physico-chemical fruit characteristics of eggplant (*Solanum melongena* L.). Food Chemistry **194**, 835–842.

Love MI, Huber W, Anders S. 2014. Moderated estimation of fold change and dispersion for RNA-seq data with DESeq2. Genome Biology **15**, 550.

Lu W, Tang X, Huo Y, Xu R, Qi S, Huang J, Zheng C, Wu CA. 2012. Identification and characterization of fructose 1,6-bisphosphate aldolase genes in Arabidopsis reveal a gene family with diverse responses to abiotic stresses. Gene **503**, 65–74.

Lupini A, Araniti F, Sunseri F, Abenavoli MR. 2013. Gravitropic response induced by coumarin: evidences of ROS distribution involvement. Plant Signaling & Behavior **8**, e23156.

Lupini A, Araniti F, Sunseri F, Abenavoli MR. 2014. Coumarin interacts with auxin polar transport to modify root system architecture in *Arabidopsis thaliana*. Plant Growth Regulation **74**, 23–31.

Lupini A, Princi MP, Araniti F, Miller AJ, Sunseri F, Abenavoli MR. 2017. Physiological and molecular responses in tomato under different forms of N nutrition. Journal of Plant Physiology **216**, 17–25.

Lv GY, Guo XG, Xie LP, *et al.* 2017. Molecular characterization, gene evolution, and expression analysis of the fructose-1, 6-bisphosphate aldolase (FBA) gene family in wheat (*Triticum aestivum* L.). Frontiers in Plant Science **8**, 1030.

Lynch JP. 2013. Steep, cheap and deep: an ideotype to optimize water and N acquisition by maize root systems. Annals of Botany **112**, 347–357.

Mandadi KK, Misra A, Ren S, McKnight TD. 2009. BT2, a BTB protein, mediates multiple responses to nutrients, stresses, and hormones in Arabidopsis. Plant Physiology **150**, 1930–1939.

Martin M. 2011. Cutadapt removes adapter sequences from high-throughput sequencing reads. EMBnet.journal **17**, 10–12.

Masclaux-Daubresse C, Daniel-Vedele F, Dechorgnat J, Chardon F, Gaufichon L, Suzuki A. 2010. Nitrogen uptake, assimilation and remobilization in plants: challenges for sustainable and productive agriculture. Annals of Botany **105**, 1141–1157.

Mauceri A, Bassolino L, Lupini A, Badeck F, Rizza F, Schiavi M, Toppino L, Abenavoli MR, Rotino GL, Sunseri F. 2020. Genetic variation in eggplant for nitrogen use efficiency under contrasting NO_3^- supply. Journal of Integrative Plant Biology **62**, 487–508.

McAllister CH, Beatty PH, Good AG. 2012. Engineering nitrogen use efficient crop plants: the current status. Plant Biotechnology Journal **10**, 1011–1025.

Mittler R, Kim Y, Song L, Coutu J, Coutu A, Ciftci-Yilmaz S, Lee H, Stevenson B, Zhu JK. 2006. Gain- and loss-of-function mutations in *Zat10* enhance the tolerance of plants to abiotic stress. FEBS Letters **580**, 6537–6542.

Moll RH, Kamprath EJ, Jackson WA. 1982. Analysis and interpretation of factors which contribute to efficiency to nitrogen utilization. Agronomy Journal **74**, 562–564.

Mulo P. 2011. Chloroplast-targeted ferredoxin-$NADP^+$ oxidoreductase (FNR): structure, function and location. Biochimica et Biophysica Acta **1807**, 927–934.

Muñoz-Bertomeu J, Cascales-Miñana B, Mulet JM, Baroja-Fernández E, Pozueta-Romero J, Kuhn JM, Segura J, Ros R. 2009. Plastidial glyceraldehyde-3-phosphate dehydrogenase deficiency leads to altered root development and affects the sugar and amino acid balance in Arabidopsis. Plant Physiology **151**, 541–558.

Nosengo N. 2003. Fertilized to death. Nature **425**, 894–895.

Pal S, Saimbhi MS, Bal SS. 2002. Effect of nitrogen and phosphorus levels on growth and yield of brinjal hybrid (*Solanum melongena* L.). Journal of Vegetable Science **29**, 90–91.

Palatnik JF, Tognetti VB, Po HO, Rodriguez RE, Blanco N, Gattuso M, Hajirezaei MR, Sonnewald U, Valle EM, Carrillo N. 2003. Transgenic tobacco plants expressing antisense ferredoxin-NADP(H) reductase transcripts display increased susceptibility to photooxidative damage. Plant Journal **35**, 332–341.

Palatnik JF, Valle EM, Carrillo N. 1997. Oxidative stress causes ferredoxin-$NADP^+$ reductase solubilization from the thylakoid membranes in methyl viologen-treated plants. Plant Physiology **115**, 1721–1727.

Portis E, Barchi L, Toppino L, *et al.* 2014. QTL mapping in eggplant reveals clusters of yield-related loci and orthology with the tomato genome. PLoS ONE **9**, e89499.

Postma JA, Dathe A, Lynch JP. 2014. The optimal lateral root branching density for maize depends on nitrogen and phosphorus availability. Plant Physiology **166**, 590–602.

Prohens J, Whitaker BD, Plazas M, Vilanova S, Hurtado M, Blasco M, Gramazio P, Stommel JR. 2013. Genetic diversity in morphological characters and phenolic acids content resulting from an interspecific cross between eggplant, *Solanum melongena*, and its wild ancestor (*S. incanum*). Annals of Applied Biology **162**, 242–257.

Qin L, Walk TC, Han P, *et al.* 2019. Adaption of roots to nitrogen deficiency revealed by 3D quantification and proteomic analysis. Plant Physiology **179**, 329–347.

Quan X, Zeng J, Ye L, Chen G, Han Z, Shah JM, Zhang G. 2016. Transcriptome profiling analysis for two Tibetan wild barley genotypes in responses to low nitrogen. BMC Plant Biology **16**, 30.

Remans T, Nacry P, Pervent M, Girin T, Tillard P, Lepetit M, Gojon A. 2006. A central role for the nitrate transporter NRT2.1 in the integrated morphological and physiological responses of the root system to nitrogen limitation in Arabidopsis. Plant Physiology **140**, 909–921.

Robert HS, Quint A, Brand D, Vivian-Smith A, Offringa R. 2009. BTB and TAZ domain scaffold proteins perform a crucial function in Arabidopsis development. Plant Journal **58**, 109–121.

Robinson MD, Oshlack A. 2010. A scaling normalization method for differential expression analysis of RNA-seq data. Genome Biology **11**, R25.

Rotino GL, Sala T, Toppino L. 2014. Eggplant. In: Pratap A, Kumar J, eds. Alien gene transfer in crop plants, Vol. 2. New York: Springer, 381–409.

Rushton PJ, Somssich IE, Ringler P, Shen QJ. 2010. WRKY transcription factors. Trends in Plant Science **15**, 247–258.

Sham A, Moustafa K, Al-Shamisi S, Alyan S, Iratni R, AbuQamar S. 2017. Microarray analysis of Arabidopsis *WRKY33* mutants in response to the necrotrophic fungus *Botrytis cinerea*. PLoS ONE **12**, e0172343.

Shen H, Liu C, Zhang Y, Meng X, Zhou X, Chu C, Wang X. 2012. OsWRKY30 is activated by MAP kinases to confer drought tolerance in rice. Plant Molecular Biology **80**, 241–253.

Siddiqi MY, Glass DM. 1981. Utilization index: a modified approach to the estimation and comparison of nutrient utilization efficiency in plants. Journal of Plant Nutrition **4**, 289–302.

Simons M, Saha R, Guillard L, Clément G, Armengaud P, Cañas R, Maranas CD, Lea PJ, Hirel B. 2014. Nitrogen-use efficiency in maize (*Zea mays* L.): from 'omics' studies to metabolic modelling. Journal of Experimental Botany **65**, 5657–5671.

Song Y, Jing SJ, Yu DQ. 2009. Overexpression of the stress induced *OsWRKY08* improves the osmotic stress tolerance in Arabidopsis. Chinese Science Bulletin **54**, 4671–4678.

Sugiura M, Georgescu MN, Takahashi M. 2007. A nitrite transporter associated with nitrite uptake by higher plant chloroplasts. Plant & Cell Physiology **48**, 1022–1035.

Sun P, Tian QY, Chen J, Zhang WH. 2010. Aluminium-induced inhibition of root elongation in Arabidopsis is mediated by ethylene and auxin. Journal of Experimental Botany **61**, 347–356.

Tanaka R, Koshino Y, Sawa S, Ishiguro S, Okada K, Tanaka A. 2001. Overexpression of chlorophyllide a oxygenase (CAO) enlarges the antenna size of photosystem II in *Arabidopsis thaliana*. Plant Journal **26**, 365–373.

Tegeder M, Masclaux-Daubresse C. 2018. Source and sink mechanisms of nitrogen transport and use. New Phytologist **217**, 35–53.

Thimm O, Bläsing O, Gibon Y, Nagel A, Meyer S, Krüger P, Selbig J, Müller LA, Rhee SY, Stitt M. 2004. MAPMAN: a user-driven tool to display genomics data sets onto diagrams of metabolic pathways and other biological processes. Plant Journal **37**, 914–939.

Toppino L, Barchi L, Lo Scalzo R, *et al.* 2016. Mapping quantitative trait loci affecting biochemical and morphological fruit properties in eggplant (*Solanum melongena* L.). Frontiers in Plant Science **7**, 256.

Tzfadia O, Bocobza S, Defoort J, *et al.* 2018. The 'TranSeq' 3′-end sequencing method for high-throughput transcriptomics and gene space refinement in plant genomes. Plant Journal **96**, 223–232.

Tzfadia O, Diels T, De Meyer S, Vandepoele K, Aharoni A, Van de Peer Y. 2016. CoExpNetViz: comparative co-expression networks construction and visualization tool. Frontiers in Plant Science **6**, 1194.

Uematsu K, Suzuki N, Iwamae T, Inui M, Yukawa H. 2012. Increased fructose 1,6-bisphosphate aldolase in plastids enhances growth and photosynthesis of tobacco plants. Journal of Experimental Botany **63**, 3001–3009.

Vandepoele K, Quimbaya M, Casneuf T, De Veylder L, Van de Peer Y. 2009. Unraveling transcriptional control in Arabidopsis using cis-regulatory elements and coexpression networks. Plant Physiology **150**, 535–546.

Viana VE, Busanello C, da Maia LC, Pegoraro C, Costa de Oliveira A. 2018. Activation of rice WRKY transcription factors: an army of stress fighting soldiers? Current Opinion in Plant Biology **45**, 268–275.

Wei Q, Wang J, Wang W, *et al.* 2020. A high-quality chromosome-level genome assembly reveals genetics for important traits in eggplant. Horticultural Research **7**, 153.

West PC, Gerber JS, Engstrom PM, *et al.* 2014. Leverage points for improving global food security and the environment. Science **345**, 325–328.

Wickham H. 2010. A layered grammar of graphics. Journal of Computational and Graphical Statistics **19**, 3–28.

Xing Y, Jia W, Zhang J. 2008. AtMKK1 mediates ABA-induced *CAT1* expression and H_2O_2 production via AtMPK6-coupled signaling in Arabidopsis. Plant Journal **54**, 440–451.

Xu G, Fan X, Miller AJ. 2012. Plant nitrogen assimilation and use efficiency. Annual Review of Plant Biology **63**, 153–182.

Yoshida S, Ito M, Nishida I, Watanabe A. 2001. Isolation and RNA gel blot analysis of genes that could serve as potential molecular markers for leaf senescence in *Arabidopsis thaliana*. Plant & Cell Physiology **42**, 170–178.

Zamboni A, Astolfi S, Zuchi S, Pii Y, Guardini K, Tononi P, Varanini Z. 2014. Nitrate induction triggers different transcriptional changes in a high and a low nitrogen use efficiency maize inbred line. Journal of Integrative Plant Biology **56**, 1080–1094.

Zhang S, Zhang A, Wu X, Zhu Z, Yang Z, Zhu Y, Zha D. 2019. Transcriptome analysis revealed expression of genes related to anthocyanin biosynthesis in eggplant (*Solanum melongena* L.) under high-temperature stress. BMC Plant Biology **19**, 387.